PCCP

Accepted Manuscript

ROYAL SOCIETY OF CHEMISTRY

www.rsc.org/pccp

Electrical Conductivity in Two Mixed-Valence Liquids

Wenzhi Yao, Steven P. Kelley, Robin D. Rogers,[1] *and Thomas P. Vaid**

Department of Chemistry, The University of Alabama, Tuscaloosa, Alabama 35487

*To whom correspondence should be addressed.

RECEIVED DATE (to be automatically inserted after your manuscript is accepted if required according to the journal that you are submitting your paper to)

[1] Current Address: Department of Chemistry, McGill University, Montreal, QC H3A 0B8

ABSTRACT. Two different room-temperature liquid systems were investigated, both of which conduct a DC electrical current without decomposition or net chemical transformation. DC electrical conductivity is possible in both cases because of the presence of two different oxidation states of a redox-active species. One system is a 1:1 molar mixture of *n*-butylferrocene (BuFc) and its cation bis(trifluoromethane)sulfonimide salt, [$BuFc^+$][NTf_2^-], while the other is a 1:1 molar mixture of TEMPO and its cation bis(trifluoromethane)sulfonimide salt, [$TEMPO^+$][NTf_2^-]. The TEMPO-[$TEMPO^+$][NTf_2^-] system is notable in that it is an electrically conducting liquid in which the conductivity originates from an organic molecule in two different oxidation states, with no metals present. Single-crystal X-ray diffraction of [$TEMPO^+$][NTf_2^-] revealed a complex structure with structurally different cation-anion interactions for *cis*- and *trans* [NTf_2^-] conformers. The electron transfer self-exchange rate constant for BuFc-$BuFc^+$ in CD_3CN was determined by ^1H NMR spectroscopy to be 5.4×10^6 $M^{-1}s^{-1}$. The rate constant allowed calculation of an estimated electrical conductivity of 7.6×10^{-5} $\Omega^{-1}cm^{-1}$ for BuFc-[$BuFc^+$][NTf_2^-], twice the measured value of 3.8×10^{-5} $\Omega^{-1}cm^{-1}$. Similarly, a previously reported self-exchange rate constant for TEMPO-$TEMPO^+$ in CH_3CN led to an estimated conductivity of 1.3×10^{-4} $\Omega^{-1}cm^{-1}$ for TEMPO-[$TEMPO^+$][NTf_2^-], a factor of about 3 higher than the measured value of 4.3×10^{-5} $\Omega^{-1}cm^{-1}$.

INTRODUCTION

Materials that are liquid at room temperature and also conduct DC electrical current (without decomposition or chemical transformation of the material) are rare. The best-known example of such a conducting liquid is elemental mercury. In addition, some amalgams (alloys) of mercury with other metallic elements are liquid at room temperature and are electrical conductors, as is gallium-indium alloy at compositions near the eutectic.

Ionic solutions and room-temperature ionic liquids will conduct an AC electrical current, but passing a direct current is possible only if faradaic processes occur at each electrode, which for most ionic solutions and ionic liquids leads to a chemical transformation or decomposition of the ions or solvent. However, if the ionic solution or ionic liquid contains a redox-active molecule or ion in two of its oxidation states, DC electrical current can pass through the solution without a net change in the composition of the liquid. When an electric potential is applied across such a liquid, oxidation (of the reduced species) occurs at one electrode, reduction (of the oxidized species) occurs at the other electrode, and current is carried through the bulk of the solution by electron transfer between the oxidized and reduced molecules or ions, with no net change in composition. Such solutions have been employed in semiconductor photoelectrochemical cells,[1] where the solution-phase redox couple serves both to set the electrochemical potential of the solution and to transport either electrons or holes through the solution to a counter-electrode. In the well-known TiO_2 dye-sensitized solar cell[2] the iodide/triiodide redox couple is most commonly used for this purpose.[3]

The electrical conductivity of a solution containing two oxidation states of a redox-active molecule/ion is directly proportional to the rate of electron transfer between the two species (oxidized and reduced), and that rate is first order in both the concentration of the reduced species and the concentration of the oxidized species. For a given redox couple, therefore, the electrical conductivity of a solution scales with the square of the total concentration of the redox-active species (in either oxidation state; this assumes that the ratio of oxidized/reduced species remains constant). The highest

possible conductivity occurs when there is no solvent at all, and a mixture of the two oxidation states of the redox-active molecule is itself a liquid. Two such systems are described herein.

There is some precedent for solventless, liquid, mixed-valence redox systems. Murray and co-workers have investigated $[Ru(bipy')_3]^{2+}$ (bipy' = 2,2'-bipyridine with attached polyethyleneglycol chains) molten salts in which $[Ru(bipy')_3]^{+}$ or $[Ru(bipy')_3]^{3+}$ was introduced voltammetrically.[4,5] The same group has studied mixed-valence cobaltocene[6] and viologen[7] redox couples with attached polyethyleneglycol chains, which convert the materials to viscous liquids. An ionic liquid has been created from a mixture of $[BMI][FeCl_4]$ and $[BMI]_2[FeCl_4]$ (BMI = butylmethylimidazolium), which contains both Fe^{2+} and Fe^{3+}, but it was not investigated electrochemically.[8] Finally, room-temperature molten iodide/polyiodide salts are known[9] and have been investigated more recently[10] as possible replacement redox couples for dye-sensitized solar cells, as has a $SeCN^-/(SeCN)_3^-$ based ionic liquid.[11] There are additional known ionic liquids containing derivatized ferrocenium[12] or cobaltocenium[6,12] as their cations (or with a cationic moiety covalently bound to ferrocene[13]), but these systems contained only one oxidation state of the redox-active entity.

We have investigated two simple systems in which there are two stable oxidation states, and electron transfer occurs between the two by an outer-sphere mechanism. One is based on the classic organometallic complex ferrocene, which is chemically stable in the neutral and +1 charged states. Both ferrocene and common ferrocenium salts are solids at room temperature, but adding alkyl substituents to one or both cyclopentadienyl rings decreases the melting point; the derivative examined for this study, *n*-butylferrocene (Figure 1), is a liquid at room temperature. The other system we have studied is the stable organic free radical (2,2,6,6-tetramethylpiperidin-1-yl)oxy (TEMPO, Figure 2). Neutral TEMPO

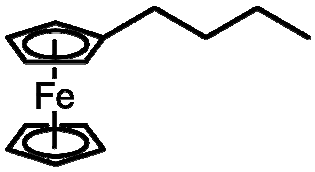

Figure 1. *n*-Butylferrocene.

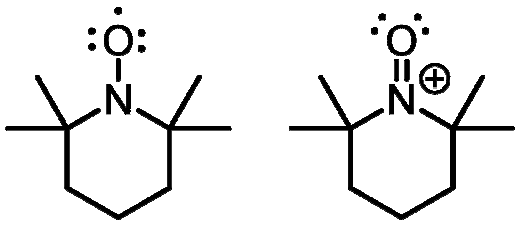

Figure 2. The TEMPO radical and cation.

is an odd-electron species that is stable at room temperature and is not air-sensitive. TEMPO can be oxidized to $TEMPO^+$ (see Figure 2), and the cation is also moderately stable in air. While neutral TEMPO is a solid at room temperature (m.p. 36-38 °C), when mixed with an appropriate $TEMPO^+$ salt (as discussed herein), the mixture is a liquid at room temperature.

EXPERIMENTAL SECTION

General procedures and materials. Reagents were purchased from commercial suppliers and used as received, unless noted as follows. CH_3CN was distilled from P_2O_5, stored over activated 3 Å molecular sieves, and vacuum transferred for use. CH_2Cl_2 was distilled from P_2O_5, stored over CaH_2, and vacuum transferred for use. The syntheses of $[BuFc^+][OTf^-]$ and $[BuFc^+][NTf_2^-]$ were carried out under a nitrogen atmosphere with dried solvents, and the products were stored in a nitrogen-filled glovebox. Differential scanning calorimetry (DSC) was measured on a Mettler-Toledo Star DSC1 system. DSC scans were conducted at a ramp rate of 5 °C/min with 10 min isotherms at the end of each dynamic heating or cooling step.

$[BuFc^+][OTf^-]$. *n*-Butylferrocene (1.000 g, 4.130 mmol), AgOTf (1.280 g, 4.982 mmol), and 10 mL of CH_3CN were combined to form a deep blue solution, which was stirred at 22 °C for 30 minutes. A light gray precipitate formed during the reaction. The CH_3CN was removed under vacuum and 10 mL of CH_2Cl_2 was added and then removed under vacuum (to precipitate excess AgOTf). New CH_2Cl_2 (10 mL) was added and the suspension was filtered. Volatiles were removed from the filtrate under vacuum to yield a dark blue, viscous oil, which was stored in an N_2-filled glovebox. Yield: 1.602 g, 99 %. ^1H NMR (CD_3CN): δ 35.79 (br, 2 H), δ 32.23 (br, 2 H), δ 29.72 (br, 5 H), δ 1.92 (br, 2 H), δ -0.21 (br, 3 H), δ -6.15 (br, 2 H), δ -18.98 (br, 2 H). ^{13}C NMR (CD_3CN, partial spectrum): δ 305.2, 260.0, 139.5, 17.0, 13.4, 5.7. UV-vis (acetonitrile, λ_{max}, nm): < 200, 255, 620.

$[BuFc^+][NTf_2^-]$. *n*-Butylferrocene (100 mg, 0.413 mmol), $AgNO_3$ (70.2 mg, 0.413 mmol), $LiNTf_2$ (118.6 mg, 0.413mmol), and 10 mL of CH_3CN were combined to form a deep blue solution, which was

stirred at 22 °C for 30 minutes. A light gray precipitate formed. The CH_3CN was removed under vacuum, 10 mL of CH_2Cl_2 was added and the suspension stirred, and the volatiles were then removed under vacuum. A fresh aliquot of 10 mL of CH_2Cl_2 and the suspension was filtered. Volatiles were removed from the filtrate under vacuum to yield a dark blue, viscous oil, which was stored in an N_2-filled glovebox. Yield: 210 mg, 97 %. ^{1}H NMR (d_6-acetone): δ 35.65 (br, 2 H), δ 32.71 (br, 2 H), δ 29.87 (br, 5 H), δ 1.30 (br, 2 H), δ -0.83 (br, 3 H), δ -6.11 (br, 2 H), δ -17.05 (br, 2 H). UV-vis (acetonitrile, λ_{max}, nm): 202, 255, 634.

[TEMPO$^+$][NTf$_2^-$]. TEMPO (1.000 g, 6.400 mmol) and 24 mL of H_2O were combined to form a suspension with a yellow-orange liquid phase. Concentrated HCl (*aq*) (2.2 mL, 27 mmol of HCl) was added, whereupon the suspension darkened. With stirring, 6.00 g of 6% NaClO (*aq*) (4.84 mmol of NaClO) was added. After stirring for 30 min, an orange homogeneous solution had formed. A separate solution of $LiNTf_2$ (2.000 g, 6.97 mmol) in 10 mL of H_2O was added dropwise, and a bright yellow precipitate formed immediately. The mixture was filtered and washed with 2 × 20 mL of H_2O. The bright yellow powder was allowed to dry in the ambient atmosphere. The product was stored with protection from light in an N_2-filled glovebox. Yield: 2.430 g, 87%. ^{1}H NMR (CD_3CN): δ 2.49 (br, 4 H), δ 2.41 (br, 2 H), δ 1.66 (br, 12 H). UV-vis (acetonitrile, λ_{max}, nm): < 200, 245, 453 m.p. 111-113 °C.

Crystal structure determination of [TEMPO$^+$][NTf$_2^-$]. Single crystals were grown by allowing a liquid mixture of 1:1 [TEMPO][NTf_2]:TEMPO to stand in a sealed screw-top glass vial at 19 ^{o}C for several days. Small, yellow-green tablets were formed in equilibrium with a liquid phase. A single crystal measuring 0.13x0.10x0.02 was isolated in Paratone-N oil (Hampton Research, Aliso Viejo, CA) and mounted on a Nylon loop.

Data was collected on a Bruker diffractometer equipped with a Platform 3-circle goniometer and an APEX-II CCD area detector (Bruker-AXS, Inc., Madison, WI) using graphite-monochromated Mo-Kα radiation. The crystal was cooled to 100 K under a cold nitrogen stream during collection using an N-

Helix cryostat (Oxford Cryosystems, Oxford, UK). A hemisphere of unique data was collected using a strategy of omega scans with 0.5° frame widths. Data collection, unit cell determination, data reduction, integration, scaling, and absorption correction were performed using the Apex2 software suite from Bruker.[14]

The crystal structure was solved by direct methods. Non-hydrogen atoms were located from the difference map and refined by full-matrix refinement against F^2. Hydrogen atoms were placed in calculated positions, and their coordinates were allowed to ride on the carrier atom. Hydrogen atoms on methyl groups were refined using a riding rotating model. Space group determination and ORTEP plot generation were performed using SHELXTL-97.[15] Structure solution and refinement were performed using SHELX-2013.[16] Short contact analysis and packing diagrams were made using Mercury from the CCDC.[17] CSD searches were performed using ConQuest from the CCDC.[18]

Conductivity measurements. The electrical conductivity of the liquids was measured in an open-top container made by compressing several pieces of material together in a C-clamp, as shown in Figure 3. Outer pieces of polyoxomethylene provide structural support, then copper plates for electrical connection, and finally inert platinum foil for contact with the liquids, with the platinum thereby forming two walls of the container. The central part of the liquid-containing compartment was constructed from a 3.0 mm thick piece of polytetrafluoroethylene (PTFE) with a 6.0 mm wide by 13.0 mm high notch cut out.

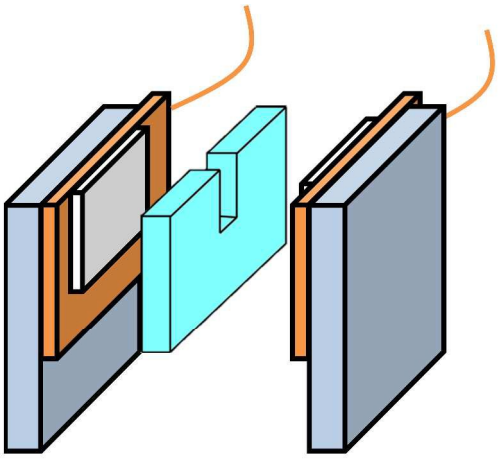

Figure 3. Container for the measurement of liquid conductivity. Materials (from outside in) are polyoxomethylene, copper, platinum, and PTFE.

With the measured mass of a liquid added to the apparatus and an estimate of its density, the volume can be determined and the area of each Pt electrode in contact with the rectangular parallelepiped of liquid can be calculated. With the known thickness (3.0 mm), measured conductance can be converted

to conductivity of the liquid. Measurements for BuFc/$BuFc^+$ mixtures were made at 22 °C under an N_2 atmosphere, while measurements for TEMPO/$TEMPO^+$ were made at 43 °C in a system open to ambient air.

RESULTS AND DISCUSSION

Synthesis and spectroscopic characterization of [$BuFc^+$][OTf^-], [$BuFc^+$][NTf_2^-] and [$TEMPO^+$][NTf_2^-]. *n*-Butylferrocenium triflate ([$BuFc^+$][OTf^-]) was synthesized by the oxidation of *n*-butylferrocene with AgOTf in CH_3CN. The product was separated from the grey precipitate of Ag^0 and excess AgOTf by dissolution in CH_2Cl_2 and filtration, followed by evaporation of the solvent to yield a dark blue oil. Because $BuFc^+$ is paramagnetic, the ^1H NMR spectrum of [$BuFc^+$][OTf^-] exhibits broadened peaks that are significantly shifted from the normal chemical shift range. The cyclopentadienyl protons have chemical shifts between 29 and 36 ppm, while the butyl protons resonate between -19 and 6.2 ppm. The UV-visible absorption spectrum has absorbances at 255 and 620 nm, similar to the reported spectrum of the ferrocenium cation.[19]

While all NMR experiments to determine self-exchange rates of Fc-Fc^+ were performed on [$BuFc^+$][OTf^-], it was found not to be completely miscible with *n*-butylferrocene at room temperature. Therefore, *n*-butylferrocenium bis(trifluoromethanesulfonyl)imide ([$BuFc^+$][NTf_2^-]) was synthesized. The oxidation of n-butylferrocene with silver nitrate in the presence of lithium bis(trifluoromethanesulfonyl)imide in acetonitrile yielded [$BuFc^+$][NTf_2^-], as shown in eq 1. Filtration in CH_2Cl_2 removed the insoluble $LiNO_3$ and Ag^0.

$$BuFc + LiNTf_2 + AgNO_3 \rightarrow [BuFc^+][NTf_2^-] + LiNO_3 + Ag^0 \quad (1)$$

The $TEMPO^+$ salt [$TEMPO^+$][NTf_2^-] (NTf_2^- = bis(trifluoromethane)sulfonimide) was synthesized by the oxidation of TEMPO with sodium hypochlorite and aqueous hydrochloric acid, by the reaction

given in eq 2. The preparation is based on previously reported preparation of several $TEMPO^+$ salts,[20] but different from the reported preparation of $[TEMPO^+][NTf_2^-]$ itself. Sodium hypochlorite in the

$$2\ TEMPO\ +\ NaOCl\ +\ 2\ HCl\ \rightarrow\ 2\ [TEMPO^+][Cl^-]\ +\ NaCl\ +\ H_2O \qquad (2)$$

presence of hydrochloric acid served as the oxidant, and addition of an aqueous solution of $LiNTf_2$ resulted in a bright yellow precipitate of $[TEMPO^+][NTf_2^-]$. The $TEMPO^+$ cation is diamagnetic and should display a normal ^1H NMR spectrum. However, we consistently obtained ^1H NMR spectra with somewhat broadened peaks, though they were still in the normal chemical shift range for those protons (1.6-2.5 ppm). The broadening is likely due to the presence of trace amounts of the neutral TEMPO radical and the electron-exchange broadening that results. The UV-visible absorption spectrum of $[TEMPO^+][NTf_2^-]$ consists of a weak absorption at 455 nm, another at 248 nm, and a strong absorption that peaks at a wavelength less than 200 nm. It seems that the 248 nm absorption is not likely due to residual neutral TEMPO (which has an absorption with a λ_{max} of 242 nm in CH_3CN), as other reported spectra of $TEMPO^+$ contain a similar peak.[21]

Crystal structure of $[TEMPO^+][NTf_2^-]$. Single crystals of $[TEMPO^+][NTf_2^-]$ were obtained from a liquid mixture of $[TEMPO^+][NTf_2^-]$ and TEMPO upon standing in a sealed container at 19 °C for several days. $[TEMPO^+][NTf_2^-]$ was found to crystallize in P-1 with Z = 8. The high Z' observed here is likely the result of the conformational freedom of the anions, where one *cis* conformation and three *trans* (3) conformations (differing by the positions of the $-CF_3$ groups) are observed (Figure 4, bottom). Examination of the short (less than the sum of the van der Waals radii) contacts around each ion reveals that the *cis* anion has a particularly large number of contacts with one cation. One of the *trans* anions likewise is found to interact particularly strongly with one cation. These two cation-anion pairs further dimerize with each about crystallographic centers of symmetry other to form clusters of two anions and two cations (Figure 5). Since the crystals from which this structure was determined were formed directly from the melt, in accordance with Ostwald's rule they are likely to be the highest energy polymorph.[22]

Such polymorphs can crystallize because they incorporate the supramolecular assemblies found in the liquid state, whereas the more thermodynamically stable polymorphs are kinetically disfavored because they require disassembly of those structures before the individual molecules can be incorporated into the crystal.[23] It therefore seems plausible that in this crystal two of the most common ion pairs from the liquid state have been trapped, one cation-anion pair for the anion in its *trans* conformation and one for its *cis* conformation, with the other two symmetry-inequivalent cations and anions appearing to act as a sort of crystallographic mortar which binds the most closely bound ion clusters together.

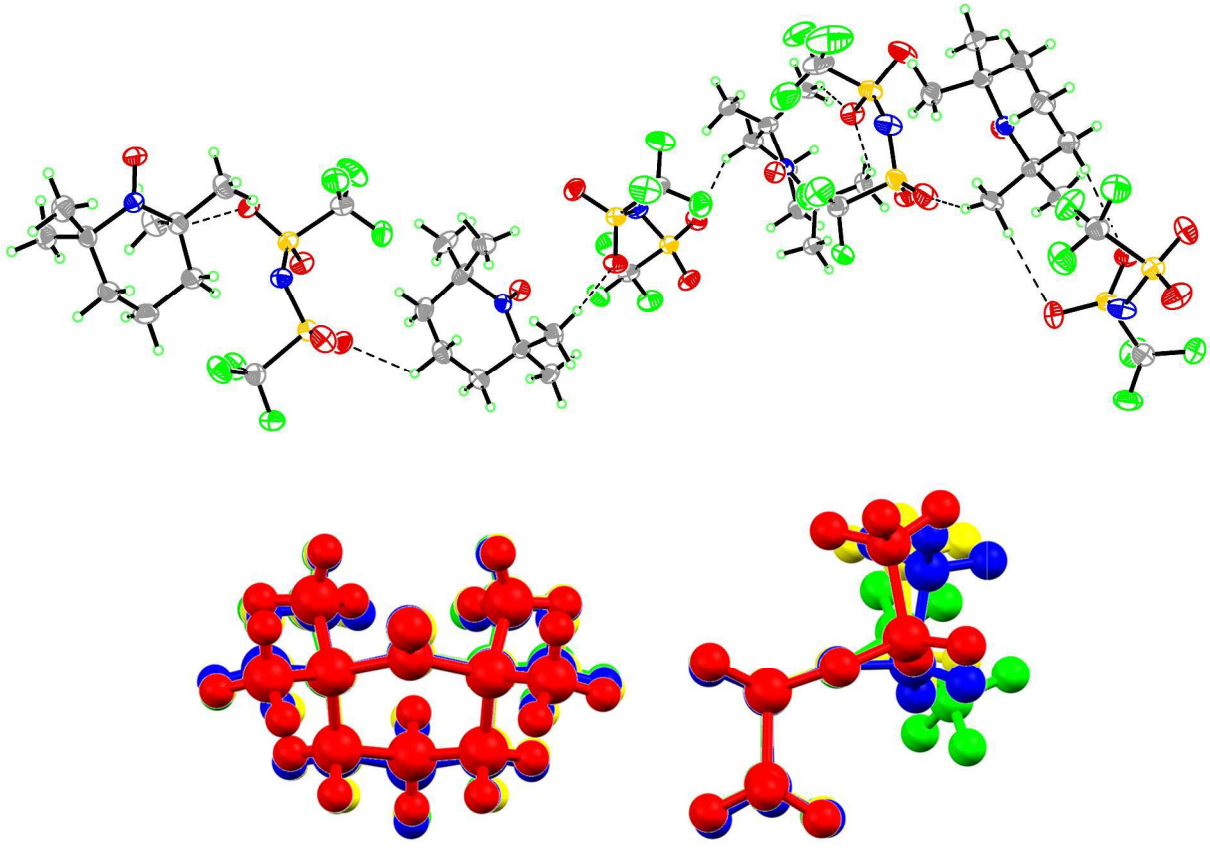

Figure 4. Top: 50% probability ellipsoid diagram of the asymmetric unit of [TEMPO$^+$][NTf$_2^-$] showing the shortest intermolecular contacts (expressed as dashed lines). Bottom: Overlays of all symmetry unique cations (left) and anions (right) colored to distinguish atoms on different molecules. *Cis*-conformer anion is in green.

The *cis* conformation of the [NTf$_2^-$] anion is uncommon in crystal structures of organic salts because the *trans* conformation is more stable, but it does occur when stabilized by coordination to a metal ion or specific intermolecular interactions with an organic counterion.[27] No other organic crystals

containing both *cis* and *trans* conformations of $[NTf_2]^-$ could be found in the CSD.[24] Interestingly, while the S-C bond distances are slightly shorter in the *cis* anion than the other three, all S-O and S-N bond distances are similar within experimental error and the C-F bond distances vary unsystematically from 1.317(5) to 1.340(5) Å. The anion bond distances are similar to those observed in crystal structures of alkylated pyrrolidinium and imidazolium salts, although the dissymmetry of the C-S bonds is somewhat greater than usually reported.[25–28]

The asymmetric unit contains four structurally similar, but symmetry-independent cations each in a chair conformation (Figure 4). The N-O bond distances range from 1.190(3) to 1.198(4) Å, which is significantly shorter than the N-O bond distances in salts of the TEMPO cation with more coordinating anions such as Cl^- and BF_4^-.[29,30] N1 and the three atoms to which it is bonded, C1, C5, and O1, are very nearly coplanar (mean deviations from the least squares plane range = 0.0002 - 0.005 Å). The N1-centered bond angles are close to 120°, with the C-N-C bond angles being wider and both O-N-C bond angles being a little shorter. These features indicate trigonal planar geometry around the nitrogen atoms, slightly distorted by the geometry of the ring, with the N-O double bond relatively unperturbed by intermolecular interactions.

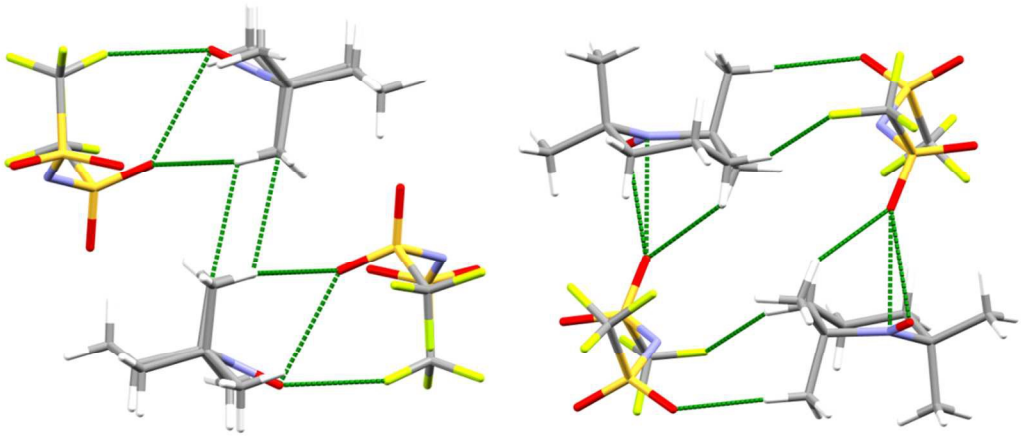

Figure 5. Packing diagrams of the *cis*-anion cation cluster (*left*) and the *trans*-anion-cation cluster (*right*). Green lines indicate short contacts.

Thermal characterization. Our goal was to create mixed-valence materials that are liquid at room temperature. *n*-Butylferrocene (BuFc) was a promising starting point since it is a liquid at room temperature, with a reported melting point of 7 °C.[12] We performed DSC measurements on BuFc and it shows reproducible supercooling and undergoes an exothermic solid-to-solid transition with T_{onset} = -49.0(5) °C and melting with T_{onset} = 6.94(1) °C, similar to the published value for the melting point. [$BuFc^+$][NTf_2^-] is known and has a reported glass transition temperature (without a sharp melting point) of -81 °C.[12] We found that [$BuFc^+$][NTf_2^-] is a liquid at room temperature, and it is completely miscible with BuFc. A 1:1 molar mixture of BuFc and [$BuFc^+$][NTf_2^-] is, as expected, a liquid at room temperature.

TEMPO is a solid at room temperature, but with a low melting point of 36-38 °C. The melting point of [$TEMPO^+$][NTf_2^-] is 111-113 °C. A 1:1 molar mixture of TEMPO and [$TEMPO^+$][NTf_2^-] is a room-temperature liquid: DSC (Figure 10) shows that the liquid 1:1 mixture crystallizes upon cooling and has a melting onset that occurs at 13.7(5) °C. The mixture also shows hysteresis on cooling with multiple crystallization events occurring on the third cooling cycle, possibly due to the formation of different crystalline products on different cooling cycles. [$TEMPO^+$][NTf_2^-] crystallized from the 1:1 mixture on standing for several days at 19 °C.

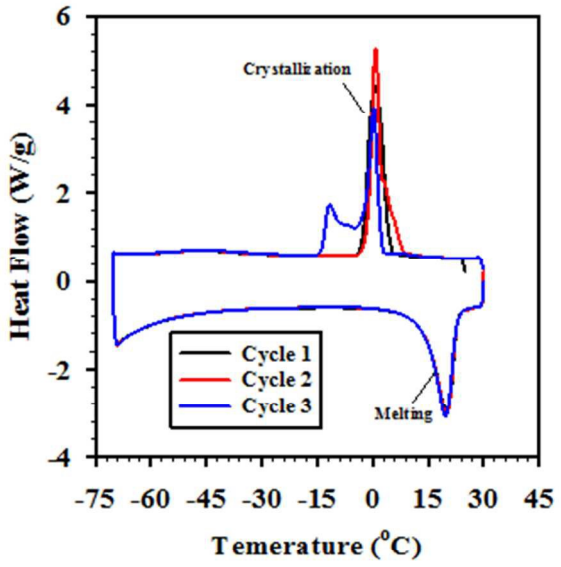

Figure 6. DSC of 1:1 TEMPO-[$TEMPO^+$][NTf_2^-].

This approach, in which ionic and neutral compounds are combined to achieve extreme melting point depression, has been used in the design ILs and IL-like systems. It is often considered to be due to the formation of new species rather than the typical melting point depression observed when combining solids.[31] Examples include combining neutral hydrogen bond donors with salts to increase the effective size of the anion and form deep eutectic solvents,[32] combining salts with neutral conjugate acids or

bases of one of the ions to form larger, oligomeric ions,[33,34] or reacting acids and bases that remain strongly associated rather than undergoing full ionization.[35] The combination of [TEMPO$^+$][NTf$_2^-$] with TEMPO parallels this approach, but the interaction between TEMPO and [TEMPO$^+$] is not mediated by proton transfer. If the two are able to form an oligomeric ion, it would be a novel case in which the charge is delocalized across both molecules by electron transfer rather than proton transfer.

Electron transfer self-exchange rates and predicted conductivity. The self-exchange electron transfer between a molecule M and its cation M$^+$ in solution is given by eq 3, and the rate of the self-exchange reaction is given by eq 4. With a known rate constant k_{ex} for a self-exchange reaction, it is possible to calculate an estimated electrical conductivity for a mixture of the M and M$^+$ species.[7,36] We have therefore determined the self-exchange rate for BuFc/BuFc$^+$ by NMR spectroscopy. This has been done previously for ferrocene[37–40] and various alkylated ferrocenes,[38,39] but never for *n*-butylferrocene.

$$M + M^+ \rightarrow M^+ + M \tag{3}$$

$$\text{rate} = k_{ex}[M][M^+] \tag{4}$$

The trifluoromethanesulfonate salt of BuFc, [BuFc$^+$][OTf$^-$], was used in the NMR self-exchange rate experiments, while [BuFc$^+$][NTf$_2^-$] was used to create the BuFc/BuFc$^+$ mixed-valence liquid because BuFc and [BuFc$^+$][OTf$^-$] were found to not be completely miscible at room temperature. The BuFc/BuFc$^+$ self-exchange rate in acetonitrile will be nearly identical for the two anions.

NMR spectra of pure BuFc and pure [BuFc$^+$][OTf$^-$] in CD_3CN were obtained. Then a spectrum of a mixture that was 0.0498 M in [BuFc$^+$][OTf$^-$] and 0.0491 M in BuFc in CD_3CN was obtained. The self-exchange rate was calculated by using eq 5,[39]

$$k = \frac{4\pi x_D x_P \delta_v{}^2}{(W_{DP} - x_P W_P - x_D W_D)c_{tot}} \tag{5}$$

where χ_D and χ_P are the mole fractions of diamagnetic and paramagnetic species (in this case BuFc and BuFc$^+$), respectively, δ_v is the difference in resonance frequency (in hertz) between the pure diamagnetic and paramagnetic samples, W_{DP}, W_P, and W_D are the NMR line widths (in hertz) at half-height for

mixed, pure paramagnetic, and pure diamagnetic samples, respectively, and C_{tot} is the total concentration (paramagnetic + diamagnetic) in the mixed sample (in mol/L). The resonance used for the calculations was the singlet due to the unsubstituted cyclopentadienyl ring. Line widths were determined with the Bruker TOPSPIN software using a mixed Lorentzian and Gaussian lineshape. For BuFc/BuFc$^+$ the self-exchange rate constant at 25 °C determined using eq 5 was 5.4 × 10^6 M^{-1}s^{-1}. Previously reported values for the self-exchange rate for Fc/Fc$^+$ in CD_3CN at 25 °C are 5.3 × 10^6 M^{-1}s^{-1}, 7.1-9.1 × 10^6 M^{-1}s^{-1}, and 7.8-9.3 × 10^6 M^{-1}s^{-1}.[37,39,40] The value of 5.3 × 10^6 M^{-1}s^{-1},[37] however, was later shown[39] to likely be too low. The correct value is therefore likely 7-9 × 10^6 M^{-1}s^{-1}. The exchange rate for di(n-butylcyclopentadienyl)iron is slightly lower than that of Fc/Fc$^+$,[38] so our measured value of 5.4 × 10^6 M^{-1}s^{-1} for BuFc/BuFc$^+$ is reasonable.

A previously reported model[7,36,41] of conductivity through a cubic lattice of mixed-valence redox species allows the calculation of a predicted conductivity based on the self-exchange rate k_{ex} and concentrations of the oxidized and reduced forms of the redox species. To perform the calculation, the density of the BuFc-[BuFc$^+$][NTf_2^-] mixture must be measured or estimated. The density of 1:1 BuFc-[BuFc$^+$][NTf_2^-] was estimated to be 1.54 g/cm^3 based on the published density of 1.172 g/cm^3 for BuFc and an estimated density of 1.8 g/cm^3 for [BuFc$^+$][NTf_2^-]. The concentrations of BuFc and BuFc$^+$ in this solventless 1:1 mixture can then be calculated: each is 2.0 M. The average Fe-Fe distance was calculated to be 7.46 Å. With this information the conductivity of 1:1 BuFc-[BuFc$^+$][NTf_2^-] is predicted[7,36] to be 7.6 × 10^{-5} Ω^{-1}cm^{-1} by this model.

We did not measure the electron-transfer self-exchange rate constant, k_{ex}, for TEMPO-TEMPO$^+$, as a value has already been published.[42] That value, however, was given as k_{et}, which is the electron-transfer rate constant within a pre-formed complex of the cation and radical. The value of k_{ex} was calculated as follows. Equation 7[42] and eq 8[43] were combined to yield eq 9.

$$\frac{1}{k_{obs}} = \frac{2}{k_{diff}} + \frac{1}{k_{et}} \qquad (7)$$

$$\frac{1}{k_{obs}} = \frac{1}{k_{diff}} + \frac{1}{K_A k_{el} \nu_n} \quad (8)$$

$$\frac{1}{k_{diff}} + \frac{1}{k_{et}} = \frac{1}{K_A k_{el} \nu_n} \quad (9)$$

The values k_{diff}, k_{et}, and $k_{el}\nu_n$ were taken from the same publication[42] as 1.90×10^{10} $M^{-1}s^{-1}$, 2.6×10^{8} $M^{-1}s^{-1}$, and 7.06×10^{6}, respectively. From this K_A was calculated to be 36.33. Finally, from eq 10 and the reported value of k_{et} (2.6×10^{8} $M^{-1}s^{-1}$),[42] the value of k_{ex} was calculated to be 7.16×10^{6} $M^{-1}s^{-1}$.

$$k_{et} = K_A k_{ex} \quad (10)$$

With the self-exchange rate constant of 7.16×10^{6} $M^{-1}s^{-1}$, a predicted conductivity for 1:1 TEMPO-[$TEMPO^+$][NTf_2^-] can be calculated using the same model as used for BuFc-[$BuFc^+$][NTf_2^-]. For [$TEMPO^+$][NTf_2^-] the density calculated from the crystal structure reported herein is 1.612 g/cm^3. Since the density of TEMPO is 1.05 g/cm^3,[44] we calculated the density of the 1:1 molar mixture of TEMPO-[$TEMPO^+$][NTf_2^-] to be 1.4 g/cm^3. That yields a concentration of 2.2 M for TEMPO and 2.2 M for $TEMPO^+$ in the 1:1 molar mixture of TEMPO-[$TEMPO^+$][NTf_2^-]. The calculated average TEMPO-TEMPO distance is 7.23 Å. With this information the conductivity of 1:1 TEMPO-[$TEMPO^+$][NTf_2^-] was predicted[7,36] to be 1.3×10^{-4} $\Omega^{-1}cm^{-1}$ in this model.

Measured DC conductivity of 1:1 BuFc-[$BuFc^+$][NTf_2^-] and 1:1 TEMPO-[$TEMPO^+$][NTf_2^-]. The conductivity of a 1:1 molar mixture of BuFc-[$BuFc^+$][NTf_2^-] was determined by adding a known mass of the liquid to the apparatus shown in Figure 3 and measuring the current at a constant applied potential at 22 °C under an N_2 atmosphere. The conductivity was calculated using eq 6,

$$\kappa = \frac{I\rho l^2}{Um} \quad (6)$$

where κ ($\Omega^{-1}cm^{-1}$) is the conductivity, I (amps) is the measured current, ρ (g/cm^3) is the estimated density of the liquid, l (cm) is the distance between the two electrodes (0.30 cm in our device), U (V) is the applied potential, and m (g) is the mass of material. The density of 1:1 BuFc-[$BuFc^+$][NTf_2^-] was

earlier estimated to be 1.54 g/cm^3. Four measurements were performed on each of the two 0.15 g samples of 1:1 BuFc-[BuFc$^+$][NTf$_2^-$]. A 1.000 V potential was applied for 24 h for each measurement, with a one hour period with no applied potential between measurements. The first measurement did not reach a steady-state current within its 24 h period (the current decreased throughout the 24 h), so that data was not used. Each of the next three reached a steady-state current within about 1 hour, and it is those steady-state current values that were used to calculate the conductivities in Table 1. The average conductivity is 3.8×10^{-5} Ω^{-1}cm^{-1}, one half the predicted value of 7.6×10^{-5} Ω^{-1}cm^{-1}.

Table 1. Measured Conductivity of BuFc-[BuFc$^+$][NTf$_2^-$] and TEMPO-[TEMPO$^+$][NTf$_2^-$] Mixtures

	Sample	Conductivity (μS·cm-1)	Average Conductivity (μS·cm-1)
BuFc / BuFc+	1	36.9	37.4
		38.5	
		36.7	
	2	38.9	38.2
		37.8	
		38.0	
TEMPO / TEMPO+	1	43.4	43.4
		43.7	
		43.0	
	2	42.3	42.4
		39.3	
		45.6	

The conductivity of 1:1 TEMPO-[TEMPO$^+$][NTf$_2^-$] was measured in the same way as for the ferrocene-based material, except that the measurements were made at 43 °C to prevent crystallization of [TEMPO$^+$][NTf$_2^-$], and in this case the sample was open to ambient air. The density of 1:1 TEMPO-[TEMPO$^+$][NTf$_2^-$] was earlier calculated to be 1.4 g/cm^3. Two samples (158 mg and 134 mg) of 1:1 TEMPO-[TEMPO$^+$][NTf$_2^-$] were used for two sets of the three measurements, with a 1.000 V potential applied for 24 hours in each measurement, with a 1 hour rest between measurements. The steady-state

currents were used to calculate the conductivities shown in the Table 1. The average value of 4.3×10^{-5} $\Omega^{-1}cm^{-1}$ is a factor of about 3 lower than the predicted value of 1.3×10^{-4} $\Omega^{-1}cm^{-1}$.

While it is gratifying that Murray's published model[7,36,41] for conductivity in mixed-valence systems agrees roughly with the measured conductivity for our two systems, in each case the conductivity was lower than the predicted value. That was particularly true for the TEMPO-[$TEMPO^+$][NTf_2^-] system, where the measured value was less than the predicted by about a factor of 3. It is not completely clear why this was the case, although a possible explanation for the TEMPO system is given below. Both liquid systems were viscous, but actual material transport does not occur when steady-state current is flowing, so viscosity should have no effect on the steady-state current and conductivity. One difference between the measurements reported herein and those by Murray and coworkers is the timescale—their measurements were generally done over a period of several seconds, whereas ours lasted for several hours and came to a steady-state current condition. Nevertheless, it seems his model should correctly describe our system.

One possible reason for decreased conductivity in the TEMPO-[$TEMPO^+$][NTf_2^-] system is partial ordering in the liquid state, with some of the [$TEMPO^+$][NTf_2^-] component sequestered in small oligomeric structures similar to that of its crystal structure (Figure 4). The solution-phase electron self-exchange rate (used to predict the conductivity of our system) is determined in a solution with a nearly random distribution and random relative orientations of TEMPO and $TEMPO^+$, while in our TEMPO-[$TEMPO^+$][NTf_2^-] system the ordering of [$TEMPO^+$][NTf_2^-] would lead to fewer TEMPO-$TEMPO^+$ close contacts and therefore a slower overall electron transfer. Even within the [$TEMPO^+$][NTf_2^-] ordered regions themselves, if a $TEMPO^+$ cation is reduced to TEMPO subsequent electron transfer will be slow because the TEMPO molecule is highly asymmetric, with the redox-active entity (the nitroxyl group) on one side, and electron transfer requires a close approach of the cationic and neutral nitroxyl groups of neighboring molecules, which requires molecular motion and is less frequent in any ordered structure.

Both the BuFc-[$BuFc^+$][NTf_2^-] and TEMPO-[$TEMPO^+$][NTf_2^-] systems are of fundamental interest because they represent simple, well-defined 1:1 mixed valence systems reduced to their essential form, with only a neutral molecule, the cationic form of that molecule, and an anion present. The TEMPO-[$TEMPO^+$][NTf_2^-] system is of particular interest because it represents a metal-free liquid that is a conductor of DC electrical current. The only other metal-free examples known to the authors are the room-temperature molten iodide/polyiodide salts[9,10] and $SeCN^-/(SeCN)_3^-$ based ionic liquid[11] mentioned in the Introduction.

CONCLUSIONS

We have demonstrated that two liquid mixed-valence systems, one organic and the other organometallic, conduct a DC electrical current. In both cases the simplest possible system has been devised, consisting of only the neutral molecule, the molecular cation, and a counterion. That corresponds to the highest possible concentration of the redox-active species, and therefore the highest possible conductivity for a mixed-valence mixture of those species.

ACKNOWLEDGMENTS

S. P. Kelley was supported by the Department of Energy Nuclear Energy University Programs (DOE-NEUP Graduate Research Fellowship DE-NE0000366)

Supporting Information: Current-voltage plots for all conductivity measurements, ^1H NMR spectra for self-exchange rate measurements for BuFc-$BuFc^+$, and UV-vis spectra.

References

(1) Tan, M. X.; Laibinis, P. E.; Nguyen, S. T.; Kesselman, J. M.; Stanton, C. E.; Lewis, N. S. *Prog. Inorg. Chem.* **1994**, *41*, 21–144.
(2) Grätzel, M. *Inorg. Chem.* **2005**, *44*, 6841–6851.
(3) Boschloo, G.; Hagfeldt, A. *Acc. Chem. Res.* **2009**, *42*, 1819–1826.
(4) Masui, H.; Murray, R. W. *Inorg. Chem.* **1997**, *36*, 5118–5126.
(5) Ranganathan, S.; Murray, R. W. *J. Phys. Chem. B* **2004**, *108*, 19982–19989.

(6) Harper, A. S.; Leone, A. M.; Lee, D.; Wang, W.; Ranganathan, S.; Williams, M. E.; Murray, R. W. *J. Phys. Chem. B* **2005**, *109*, 18852–18859.
(7) Terrill, R. H.; Hutchison, J. E.; Murray, R. W. *J. Phys. Chem. B* **1997**, *101*, 1535–1542.
(8) Sitze, M. S.; Schreiter, E. R.; Patterson, E. V.; Freeman, R. G. *Inorg. Chem.* **2001**, *40*, 2298–2304.
(9) Stegemann, H.; Rohde, A.; Reiche, A.; Schnittke, A.; Füllbier, H. *Electrochimica Acta* **1992**, *37*, 379–383.
(10) Thorsmølle, V. K.; Rothenberger, G.; Topgaard, D.; Brauer, J. C.; Kuang, D.-B.; Zakeeruddin, S. M.; Lindman, B.; Grätzel, M.; Moser, J.-E. *ChemPhysChem* **2011**, *12*, 145–149.
(11) Wang, P.; Zakeeruddin, S. M.; Moser, J.-E.; Humphry-Baker, R.; Grätzel, M. *J. Am. Chem. Soc.* **2004**, *126*, 7164–7165.
(12) Inagaki, T.; Mochida, T.; Takahashi, M.; Kanadani, C.; Saito, T.; Kuwahara, D. *Chem. Eur. J.* **2012**, *18*, 6795–6804.
(13) Kübler, P.; Sundermeyer, J. *Dalton Trans.* **2014**, *43*, 3750–3766.
(14) APEX 2 AXScale and SAINT, version 2010; Bruker AXS, Inc.: Madison, WI.
(15) Sheldrick, G. M. (2001) SHELXTL, structure determination software suite, v.6.10. Bruker AXS Inc, Madison, WI.
(16) Sheldrick, G. M. *Acta Cryst.* **2008**, *A64*, 112-122.
(17) Macrae, C. F.; Bruno, I. J.; Chisholm, J. A.; Edgington, P. R.; McCabe, P.; Pidcock, E.; Rodriguez-Monge, L.; Taylor, R.; van de Streek, J.; Wood, P. A. *J. Appl. Cryst.* **2008**, *41*, 466–470.
(18) Bruno, I. J.; Cole, J. C.; Edgington, P. R.; Kessler, M.; Macrae, C. F.; McCabe, P.; Pearson, J.; Taylor, R. *Acta Crystallogr. B* **2002**, *58*, 389–397.
(19) Trojánek, A.; Langmaier, J.; Šebera, J.; Záliš, S.; Barbe, J.-M.; Girault, H. H.; Samec, Z. *Chem. Commun.* **2011**, *47*, 5446–5448.
(20) Shibuya, M.; Tomizawa, M.; Iwabuchi, Y. *J. Org. Chem.* **2008**, *73*, 4750–4752.
(21) Israeli, A.; Patt, M.; Oron, M.; Samuni, A.; Kohen, R.; Goldstein, S. *Free Radic. Biol. Med.* **2005**, *38*, 317–324.
(22) Ostwald, W. *Z. Physik. Chem.* **1897**, *22*, 289–330.
(23) Desiraju, G. R. *J. Am. Chem. Soc.* **2013**, *135*, 9952–9967.
(24) Allen, F. H. *Acta Crystallogr. B* **2002**, *58*, 380–388.
(25) Roth, C.; Peppel, T.; Fumino, K.; Köckerling, M.; Ludwig, R. *Angew. Chem. Int. Ed.* **2010**, *49*, 10221–10224.
(26) Choudhury, A. R.; Winterton, N.; Steiner, A.; Cooper, A. I.; Johnson, K. A. *CrystEngComm* **2006**, *8*, 742–745.
(27) Holbrey, J. D.; Reichert, W. M.; Rogers, R. D. *Dalton Trans.* **2004**, 2267–2271.
(28) Forsyth, C. M.; MacFarlane, D. R.; Golding, J. J.; Huang, J.; Sun, J.; Forsyth, M. *Chem. Mater.* **2002**, *14*, 2103–2108.
(29) Yonekuta, Y.; Oyaizu, K.; Nishide, H. *Chem. Lett.* **2007**, *36*, 866–867.
(30) Stefan, S.; Belaj, F.; Madl, T.; Pietschnig, R. *Eur. J. Inorg. Chem.* **2010**, *2010*, 289–297.
(31) Abbott, A. P.; Harris, R. C.; Ryder, K. S.; D'Agostino, C.; Gladden, L. F.; Mantle, M. D. *Green Chem.* **2011**, *13*, 82–90.
(32) Abbott, A. P.; Capper, G.; Davies, D. L.; Rasheed, R. K.; Tambyrajah, V. *Chem. Commun.* **2003**, 70–71.
(33) Johansson, K. M.; Izgorodina, E. I.; Forsyth, M.; MacFarlane, D. R.; Seddon, K. R. *Phys. Chem. Chem. Phys.* **2008**, *10*, 2972–2978.
(34) Bica, K.; Rijksen, C.; Nieuwenhuyzen, M.; Rogers, R. D. *Phys. Chem. Chem. Phys.* **2010**, *12*, 2011–2017.
(35) Bica, K.; Shamshina, J.; Hough, W. L.; MacFarlane, D. R.; Rogers, R. D. *Chem. Commun.* **2011**, *47*, 2267–2269.
(36) Wuelfing, W. P.; Green, S. J.; Pietron, J. J.; Cliffel, D. E.; Murray, R. W. *J. Am. Chem. Soc.* **2000**, *122*, 11465–11472.
(37) Yang, E. S.; Chan, M.-S.; Wahl, A. C. *J. Phys. Chem.* **1975**, *79*, 2049–2052.

(38) Yang, E. S.; Chan, M.-S.; Wahl, A. C. *J. Phys. Chem.* **1980**, *84*, 3094–3099.
(39) Nielson, R. M.; McManis, G. E.; Safford, L. K.; Weaver, M. J. *J. Phys. Chem.* **1989**, *93*, 2152–2157.
(40) Kirchner, K.; Dang, S. Q.; Stebler, M.; Dodgen, H. W.; Wherland, S.; Hunt, J. P. *Inorg. Chem.* **1989**, *28*, 3604–3606.
(41) Dalton, E. F.; Murray, R. W. *J. Phys. Chem.* **1991**, *95*, 6383–6389.
(42) Grampp, G.; Rasmussen, K. *Phys. Chem. Chem. Phys.* **2002**, *4*, 5546–5549.
(43) Sutin, N. In *Prog. Inorg. Chem.*; Lippard, S. J., Ed.; John Wiley & Sons, Inc.: Hoboken, NJ, USA, 1983; Vol. 30, pp 441–498.
(44) Bordeaux, D.; Capiomont, A.; Lajzérowicz-Bonneteau, J.; Jouve, M.; Thomas, M. *Acta Crystallogr. B* **1974**, *30*, 2156–2160.